We are IntechOpen, the world's leading publisher of Open Access books
Built by scientists, for scientists

5,800
Open access books available

142,000
International authors and editors

180M
Downloads

154
Countries delivered to

Our authors are among the

TOP 1%
most cited scientists

12.2%
Contributors from top 500 universities

CLARIVATE ANALYTICS
BOOK CITATION INDEX
INDEXED

WEB OF SCIENCE™

Selection of our books indexed in the Book Citation Index
in Web of Science™ Core Collection (BKCI)

Interested in publishing with us?
Contact book.department@intechopen.com

Numbers displayed above are based on latest data collected.
For more information visit www.intechopen.com

Chapter

Performance Investigation of the Solar Membrane Distillation Process Using TRNSYS Software

Abdelfatah Marni Sandid, Taieb Nehari, Driss Nehari and Yasser Elhenawy

Abstract

Membrane distillation (MD) is a separation process used for water desalination, which operates at low pressures and feeds temperatures. Air gap membrane distillation (AGMD) is the new MD configuration for desalination where both the hot feed side and the cold permeate side are in indirect contact with the two membrane surfaces. The chapter presents a new approach for the numerical study to investigate various solar thermal systems of the MD process. The various MD solar systems are studied numerically using and including both flat plate collectors (the useful thermal energy reaches 3750 kJ/hr with a total area of 4 m^2) and photovoltaic panels, each one has an area of 1.6 m^2 by using an energy storage battery (12 V, 200 Ah). Therefore, the power load of solar AGMD systems is calculated and compared for the production of 100 L/day of distillate water. It was found that the developed system consumes less energy (1.2 kW) than other systems by percentage reaches 52.64% and with an average distillate water flow reaches 10 kg/h at the feed inlet temperature of AGMD module 52°C. Then, the developed system has been studied using TRNSYS and PVGIS programs on different days during the year in Ain Temouchent weather, Algeria.

Keywords: solar desalination, membrane distillation, photovoltaic system, solar-thermal system, cooling system

1. Introduction

Nowadays, on the world level, the demand for drinking water is in strong growth. In fact, to face the rapid increase in water demand in the irrigation and industrial sectors, as well as in the incompressible needs of the population in the large agglomerations of the various countries, highlights the research in the desalination of water as a capital due to the fact that the water scarcity increases in countries where water resources are too low in relation to population and agriculture [1].

Solar membrane distillation (SMD) was considered an appropriate water provision option in decentralized regions. For rural arid populations with less robust infrastructure availability, it is not cost effective to scale down conventional desalination technologies, such as reverse osmosis (RO) or multistage flash distillation (MSF) [2]. Moreover, MD requires less vapor space and building material quality

compared to conventional thermal distillation processes leading to potentially lower construction costs [3]. As mentioned earlier, another reason for coupling membrane distillation technology with solar energy sources is due to its high tolerance to fluctuations in operating conditions and operation with low-grade thermal energy. Since MD is operated at a similar range of temperatures obtained from low-temperature solar heaters, integration is straightforward [4]. The selection of solar collectors depends upon the location, and low-grade thermal energy-absorbing collectors like flat plate (FPC) and evacuated tubular (ETC) collectors have been considered as thermal sources for MD by many researchers. Apart from these, compound parabolic collectors (CPC), solar stills, and solar gradient ponds were also considered as thermal sources for various MD systems [5–7].

Recently, various MD processing technics have appeared as solutions that have a free energy source and diversity of membrane distillation technologies such as direct contact membrane distillation (DCMD), vacuum membrane distillation (DMV), air gap membrane distillation (AGMD), and sweeping gas membrane distillation (SGMD) [8]. According to the high-energy costs associated with existing desalination methods, there is a great demand for technologies that can use low-temperature sources like waste heat or solar energy. DCMD is the most MD config-uration technology studied due to the simplicity and ease of handling, where its energy efficiency, called the membrane thermal efficiency (MTE), is commonly related to the operating conditions [9]. In the MD process field, the DCMD process has a lower MTE against the AGMD procedure because of conduction heat losses. The mechanism functions of the AGMD systems are based on the stagnant air gap interposition between the membrane and condensation area, which leads to an inherently increase in the thermal energy efficiency of the process [10]. Conse-quently, the first patent to discuss the principle of AGMD appeared with Hassler [11] and Weyl [12] for the basics knowledge, in which the concept and behavior of AGMD systems can be found in different literature studies [13–15]. Hanemaaijer et al. [16] introduced an idea of internal heat recovery that is called memstill membrane distillation. Sequentially, Duong et al. [17, 18] conducted a study that allowed only AGMD to restore the latent heat without any external heat exchanger. Minier-Matar et al. [19] found through their study that AGMD provides a higher resistance to mass transfer and runs at low water flow.

Although recent developments in AGMD configurations, the first flat plate AGMD system was developed by the Swedish Svenska Utvecklings AB in 2016 [20], while such modules today have been manufactured and commercialized by Scarab development. Each module is made up of 10 planar cassettes with an overall mem-brane surface of 2.3 m^2 and a global capacity of 1 to 2 m^3/day of distillate water [21]. The single stage consists of injection-molded plastic frames containing two parallel membranes, feed and exit channels for warm water, and two condensing walls [20, 22]. Achmad et al. [23] developed a portable hybrid solar membrane distillation system for the production of freshwater using vacuum multi-effect MD. The total volume distillate output during the test was approximately 70 L with an approxi-mate conductivity of 4.7 µS/cm. The average distillate output rate was 11.53 L/hr. with a maximum of 15.94 L/hr. at noontime, whereas the distillate flux was in the range of 1.5 to 2.6 L/m^2 hr.

Dynamic simulation of the combined system using tools such as TRNSYS and parametric analysis enables to design of a functional system and then optimizes it. In this study by Kumar et al. [24], the application of the cogeneration system for residential households in the UAE is considered for per capita production of 4 L/day of pure water and 50 L/day of domestic hot water. The optimized cogeneration system utilizes more than 80% of the available solar energy gain and operates between 45 and 60% collector efficiencies for FPC and ETC systems, respectively.

The cogeneration operation reduces 6–16% of thermal energy demand and also enables 25% savings in electrical energy demand.

The configuration studied in this article for seawater desalination is AGMD. It is a thermal membrane process, the driving force behind the transfer being a partial pressure difference on either side of the membrane created by a temperature difference. Compared to other membrane distillation techniques, AGMD seems interesting for its aspects of low membrane wetting and the fact that there is no additional energy consumption linked to the use of an additional pump. In recent years, AGMD has experienced more sustained development, mainly in research, thanks to developments in membrane manufacturing techniques. Seawater desalination is one of the most promising fields for the application of solar thermal energy due to the coincidence, in many places of the world, of water scarcity, seawater availability, and good levels of solar radiation (like Algeria). The solar membrane distillation (SMD) is recently an under-investigation desalination process that is suitable for developing self-sufficient, small-scale applications. The use of solar energy considerably reduces operating costs. The main objective of this project is to analyze and optimize renewable-driven AGMD systems.

This objective can contribute to ensure the availability of distillate water by using the solar desalination process. In this work, a complete test rig to evaluate the performance of the membrane distillation module driven by solar energy during the flat plate and evacuated tube collector heating process is studied throughout Ain Temouchent weather, Algeria. Additionally, this study contains a comparison of different renewable energy systems integrating an air gap membrane distillation module.

2. Materials and methods

2.1 Description of the thermal system

The studied system contains the thermal energy loop, as shown in **Figure 1**. The system incorporating a flat plate collector (FPC) with an area of 4 m² providing heat *via* a freshwater heat transfer fluid to a storage tank containing 300 L with heat exchanger internal and auxiliary heaters, a pump, and a controller in differential temperature. **Figure 2** shows the total volume of daily consumption of 100 L/day and the volume of consumption in each hour of the day.
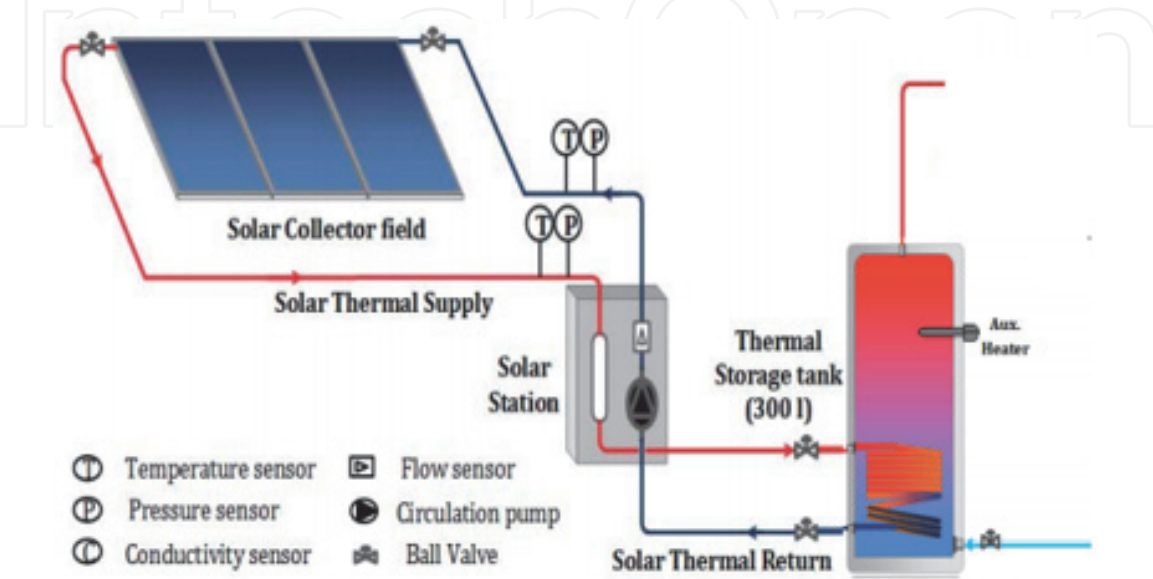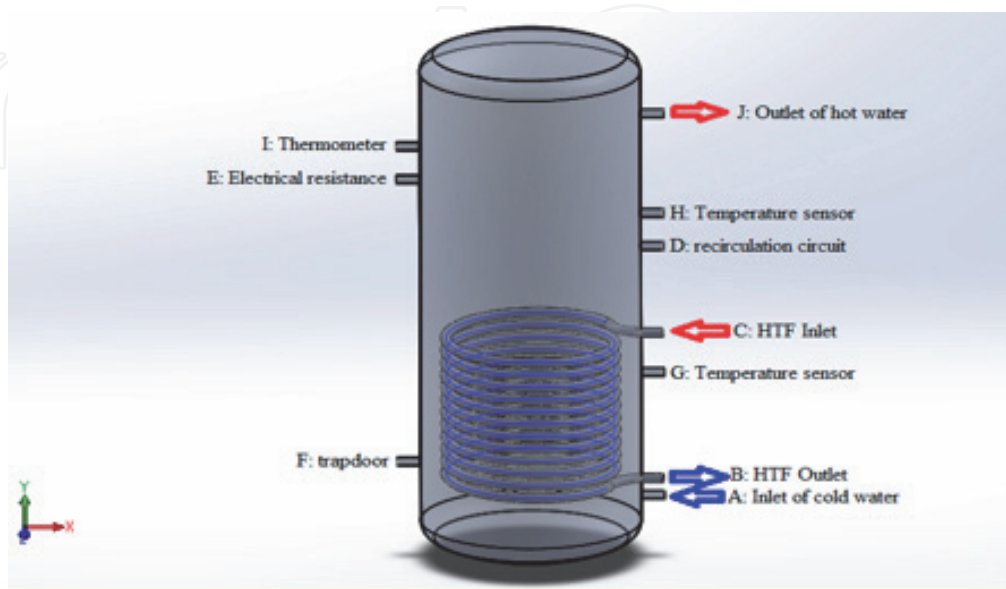

Figure 1.
Diagram of a solar hot water system.
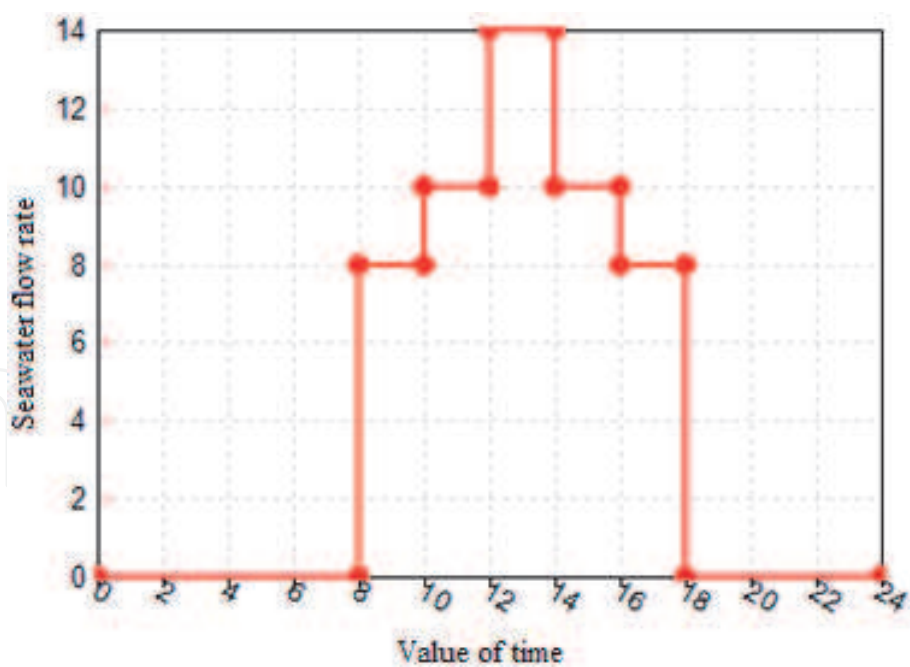
Figure 2.
*Daily seawater consumption profile (100 L/day).*

2.1.1 The thermal tank storage

The thermal tank is equipped with inlet and outlet pricking and installation of accessories, in all there are 10 prickings, the cold water inlet is at the bottom of the tank at reference A, the exit is at the top of the tank (J), the inlet of the hot fluid coming from the panel is connected to the point C and its exit to the B, in the case of a recirculating installation we use the pricking D, the auxiliary resistance is connected to the E reference, the installation of temperature probes is positioned at references G and H, the thermometer has been connected to the position I, and the point F is reserved for a manhole or a second auxiliary resistance; for more details see **Figure 3**.

Figure 3.
The thermal storage tank using SolidWorks software.
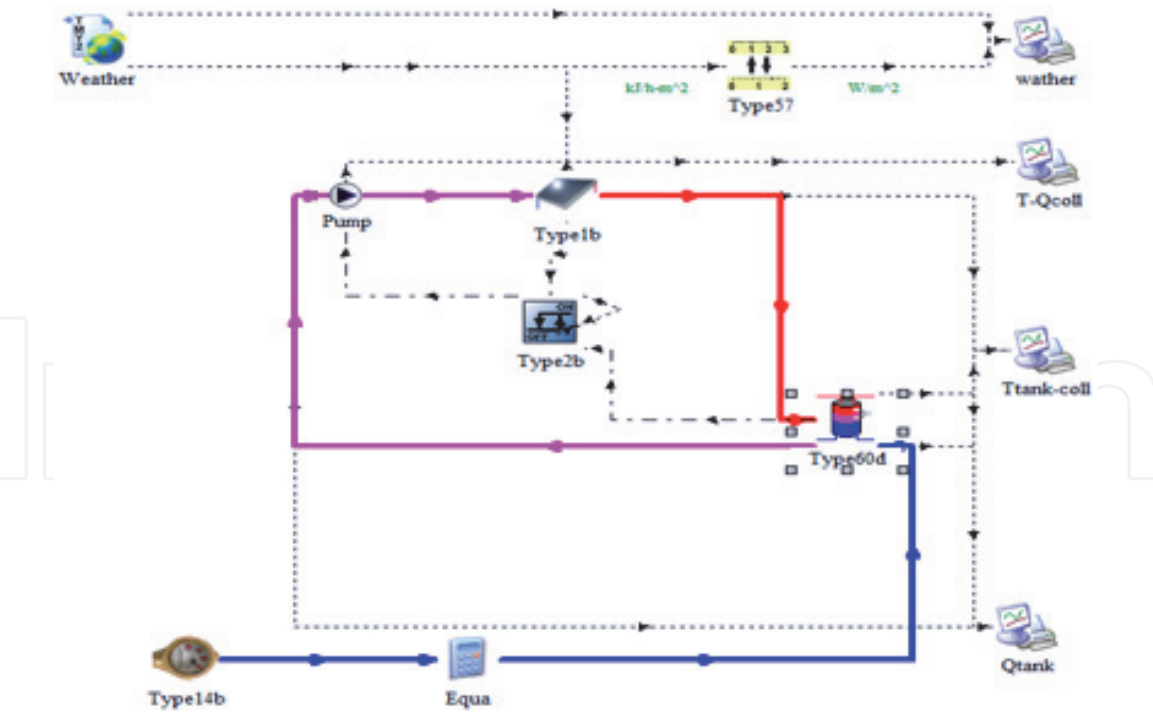
Figure 4.
Assembly diagram of the solar system in the TRNSYS simulation.

The thermal tank is completely covered with a layer of 100-mm-thick glass wool insulation and a mild steel cover sheet of 7/10 mm. A thermovitrification lining should be applied against the corrosions of the product to be heated, and a magnesium anode is installed at the top of the tank.

2.1.2 The thermal system in the TRNSYS software

The model of the solar water heating system is developed by using transient simulation software TRNSYS, as shown in **Figure 4**. The following solar system components are used:

- Reading and processing of meteorological data (TYPE109-TM2)

- Single speed pump (Type 3b)

- Flat plate collector (Type 1b)

- Storage tank with optional internal auxiliary heaters and optional internal heat exchangers with 1 input and 1 output (Type 60d)

- Distribution Water Supply Profile (Type 14e)

- Differential temperature controller (Type 2b)

- Online plotters with files (Type 65c)

The parameters of the solar system components of this model appear in **Tables 1**–**3**.

Parameters	Value	Unit
Tank volume	300	l
Tank height	1.42	m
Height of flow inlet 1	0.215	m
Height of flow outlet 1	1.415	m
Fluid specific heat	3.911	kJ/kg k
Maximum heating rate	0	kW
Heat exchanger inside diameter	0.02	m
Heat exchanger outside diameter	0.027	m
Heat exchanger fin diameter	0.027	m
Total surface area of heat exchanger	1.2	m^2
Heat exchanger length	18	m
Height of heat exchanger inlet	0.805	m
Height of heat exchanger outlet	0.215	m

Table 1.
Hot water cylinder.

Parameters	Value	Unit
Number in series	2	—
Collector absorber area	2	m^2
Intercept efficiency	0.778	kJ/kg k
inlet flow rate	20	kg/hr

Table 2.
Solar collector parameters.

Parameters	Value	Unit
Rated flow rate	20	kg/hr
Rated power	0.4	kW

**Table 3.**
Pump parameters.

2.2 The cooling system

Desalination using distillation membranes requires a very accurate study of all aspects, and because the cooling system has a significant role in the production of distilled water, in this research we study the numerical model of cooling the membrane with the use of the heat exchanger. Therefore, the power load of the heat exchanger is calculated, and the cooling system is studied with the help of the TRNSYS program in Ain Temouchent weather, Algeria.

2.2.1 Description of the cooling system

In the distillation membrane cooling unit, the distilled water tank is filled with a least half a liter and is circulated by a pump to be passed to the distillation membrane. On the opposite side, water vapor produces from the hot system. Thus, when
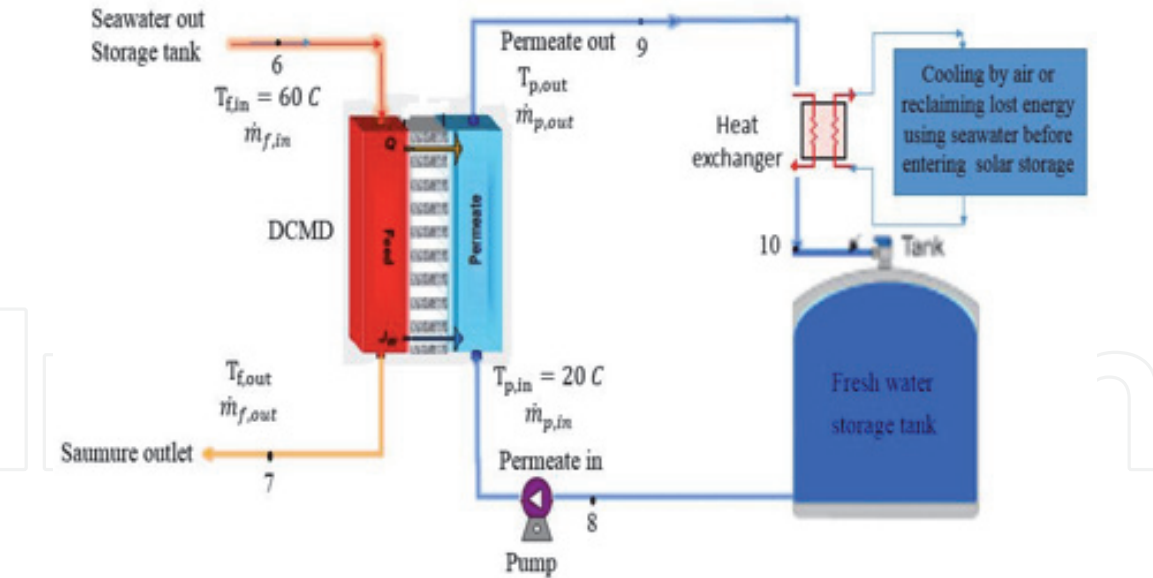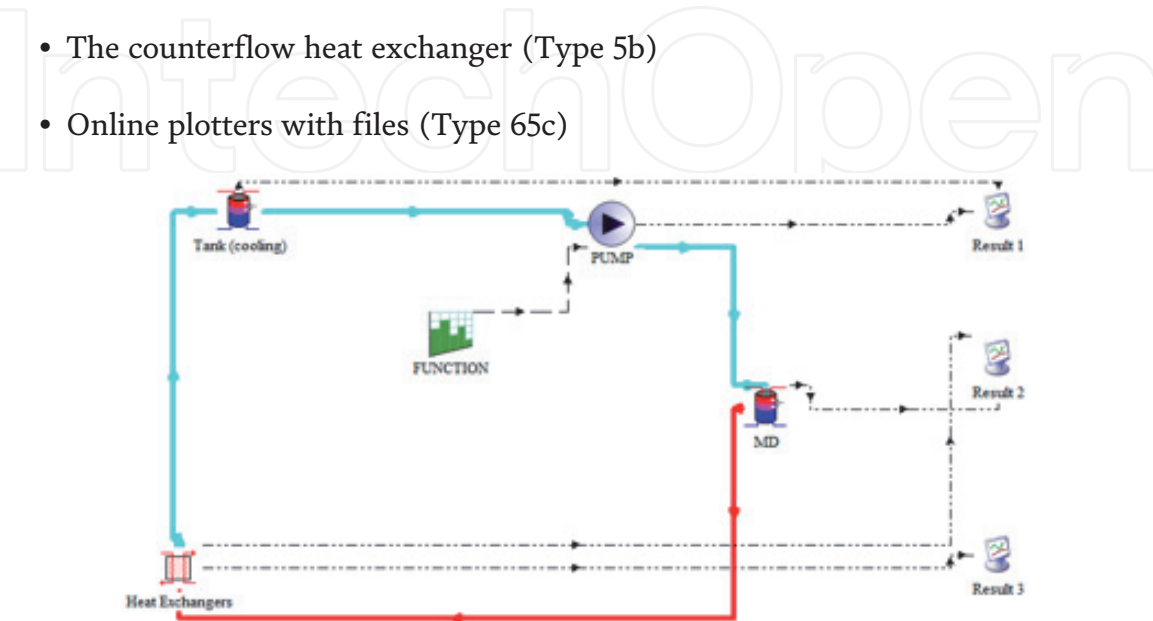
Figure 5.
Cooling system for distillation membrane.

water vapor is increased, the volume of distilled water is increased. The role of the heat exchanger is to reduce the temperature of the distilled water mixed with steam that is 50–60°C to 20–25°C. This makes the mixture state liquid "distilled water" as shown in **Figure 5**.

2.2.2 Cooling system in the TRNSYS software

A unit for cooling the distillation membrane is created at the program TRNSYS as shown in **Figure 6** with the following tools:

- Reading and processing of meteorological data (TYPE109-TM2)

- Single speed pump (Type 3b)

- Storage tank with 1 input and 1 output (Type 60d)

- The counterflow heat exchanger (Type 5b)

- Online plotters with files (Type 65c)

Figure 6.
Assembly diagram of the solar system in the TRNSYS simulation.
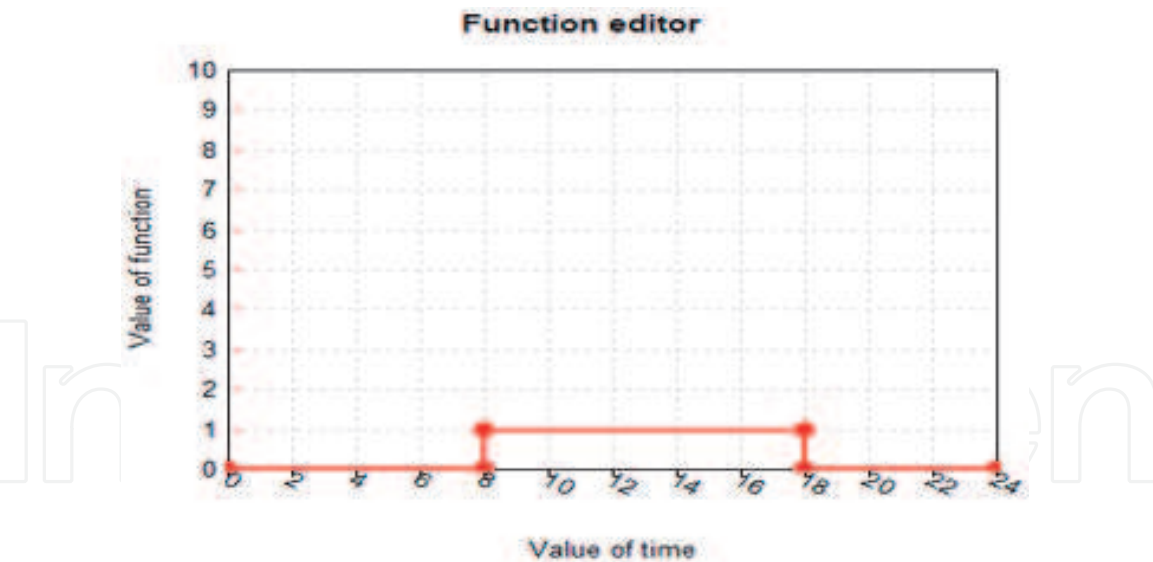
Figure 7.
*Value of time to operate cooling unit for distillation membrane.*

This system used to cool the distillation membrane relies on the heat exchanger in particular because it reduces the temperature coming out of the membrane, and thus be there more flow for distillated water and increases the production.

In order to obtain good harmonic results, we chose the time from 8 AM to 6 PM to operate the distillation membrane-cooling unit as shown in **Figure 7**. This the time when human needs in it distilled water in many fields.

2.3 Photovoltaic (PV) system

Solar PV system includes different components that should be selected according to the system type, site location, and applications. The major components for solar PV system are solar charge controller, inverter, and battery bank.

To save costs, a photovoltaic system uses based on renewable energy (solar energy). Therefore, the energy needed calculates for the pumps and replaces by photovoltaic panels, each one has an area of 1.6 m^2 by using an energy storage battery (12 V, 200 Ah). **Figure 8** presents a photovoltaic system with energy storage.
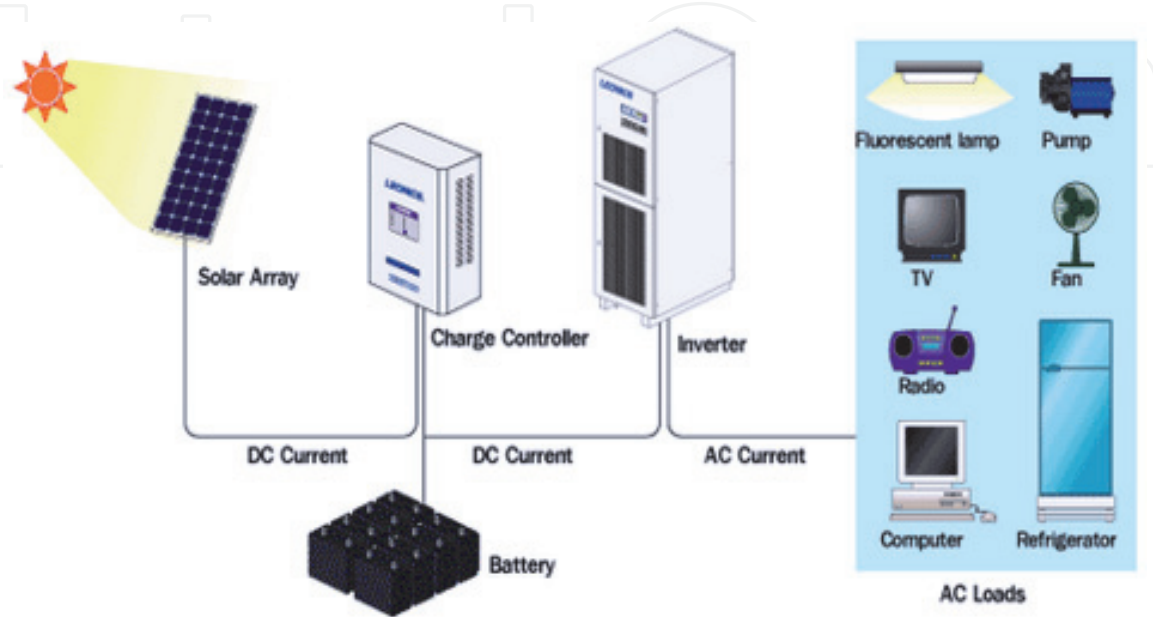
Figure 8.
Synoptic representation of the structure of a photovoltaic system with energy storage.

8

2.4 The AGMD module

AGMD is a configuration of membrane distillation (MD) in which an air layer is interposed between a porous hydrophobic membrane and the condensation surface. The module contains the cassette in a plate and frame configuration and the layout of components in the bench-scale MD module. The cassette of the AGMD module has the following specifications [24]—hydrophobic PTFE membrane with a pore size of 0.2 μm, the thickness of 280 μm, and total membrane area of 0.2 m².

3. Equations and methods

The most significant influential design variables on the AGMD performance are the feed inlet temperature (T_{Hin}), the cooling inlet temperature (T_{Cin}), which is condensation temperature, the feed flow rate (V_f), and feed concentration (C_f). The selected performance indicators of the AGMD process are distillate flux (D_w) and specific performance ratio (SPR), whereas D_w is calculated by [24]:

$$D_w = \frac{M_d}{St} \tag{1}$$

where M_d (kg) is the mass of distillate water collected within the time t and S (m²) is the effective membrane surface area of evaporation. SPR is obtained by [20]:

$$SPR = \frac{M_d}{Q_{md}} \tag{2}$$

Q_{md} (KWh) is the thermal energy supplied to the AGMD module.

The regression quadratic model with coded parameters [24] can be expressed as follows:

$$Y = \beta_0 + \beta_1 X_1 + \beta_2 X_2 + \beta_3 X_3 + \beta_{12} X_1 X_2 + \beta_{13} X_1 X_3 + \beta_{23} X_2 X_3 + \beta_{11} X_1^2 + \beta_{22} X_2^2 \\ + \beta_{33} X_3^2 \tag{3}$$

Kumar et al. [24] determined the final regression equations for D_w and T_{Hout} in terms of actual operating parameters as follows:

$$D_w = -6.57 + 0.16 \times T_{Cin} + 0.15 \times T_{Hin} - 5.86 \times 10^{-3} \times V_f - 5.77 \times 10^{-3} \\ \times T_{Cin} T_{Hin} - 2.5 \times 10^{-4} \times T_{Cin} V_f + 3.44 \times 10^{-4} \times T_{Hin} V_f + 2.48 \times 10^{-3} \\ \times T_{Hin}^2 \tag{4}$$

$$T_{Hout} = 3.097 + 6.82 \times 10^{-2} \times T_{Cin} + 0.772 \times T_{Hin} + 3.5 \times 10^{-3} \times V_f + 1.42 \times 10^{-3} \\ \times T_{Cin} T_{Hin} \tag{5}$$

The basic method of measuring collector performance is to expose the operating collector to solar radiation and measure the fluid inlet and outlet temperatures and the fluid flow rate. The useful gain is

$$\dot{Q}_u = m_0 C_{pf} (T_0 - T_i) \tag{6}$$

m_0 is the solar fluid mass flow rate (kg/hr), C_{pf} is the specific heat capacity of solar fluid (kJ/hr), and T_0 and T_i are the inlet and outlet temperatures of the solar fluid (K).

The efficiency of flat plate collectors is expressed as follows [5]:

$$\eta = \eta_0 - a_0 \times \frac{(T - T_{amb})}{G} - a_1 \times \frac{(T - T_a)2}{G} \tag{7}$$

With G the solar flux and T_a the ambient temperature, a_0 and a_1 (W/m^2 K^2) are characteristic constants of the efficiency of the collector.

Heat exchanger counterflow effectiveness is [5]:

$$\varepsilon = \frac{1 - \exp\left(-\frac{UA}{C_{min}}\left(1 - \frac{C_{min}}{C_{max}}\right)\right)}{1 - \left(\frac{C_{min}}{C_{max}}\right)\exp\left(-\frac{UA}{C_{min}}\left(1 - \frac{C_{min}}{C_{max}}\right)\right)} \tag{8}$$

UA is the overall loss coefficient between the heater and its surroundings during operation (kg/hr), C_{max} is the maximum capacity rate (kJ/hr. K), and C_{min} is the minimum capacity rate (kJ/hr. K).

Required heating rate including efficiency effects in the auxiliary heaters is [6]:

$$Q_{aux} = Q_{loss} + Q_{fluid} \tag{9}$$

With:

$$Q_{loss} = U\,A\,(\overline{T} - T_{env}) + (1 - \eta_{htr})Q_{max} \text{ and } Q_{fluid} = \dot{m}_0\,C_{pf}\,(T_{set} - T_i)$$

Q_{aux} is the required heating rate including efficiency effects (kg/hr), Q_{fluid} is the rate of heat addition to fluid stream (kg/hr), Q_{loss} is the rate of thermal losses from the heater to the environment (kg/hr), Q_{max} is the maximum heating rate of the heater (kg/hr), η_{htr} is an efficiency of the auxiliary heater, m_0 is the outlet fluid mass flow rate (kg/hr1), C_{pf} is the fluid specific heat (kJ/hr), T_i is the fluid inlet temperature (K), $(\overline{T})$ is the brackish water average temperature, T_{set} is the set temperature of heater internal thermostat (K), and T_{env} is the temperature of heater surroundings for loss calculations (K).

The PV system is calculated the following equations [7]:

The peak power of the autonomous photovoltaic installation is

$$P_c = P_{pv} = \frac{D}{N \times F} \tag{10}$$

Pc Power of the PV field, *D* Daily need kWh/day, *F* Form factor, *N* Number of hours equivalent.

$$N = \frac{G_T(t)}{G_{T,STC}} \tag{11}$$

$G_T(t)$ is the solar radiation incident on the solar PV array in the current time step kW/m^2; $G_{T,STC}$ is the incident radiation at standard test conditions kW/m^2.

4. The solar AGMD system

The model of the solar thermal AGMD system is developed by using TRNSYS software, which is a quasi-steady-state simulation program. TRNSYS is a transient
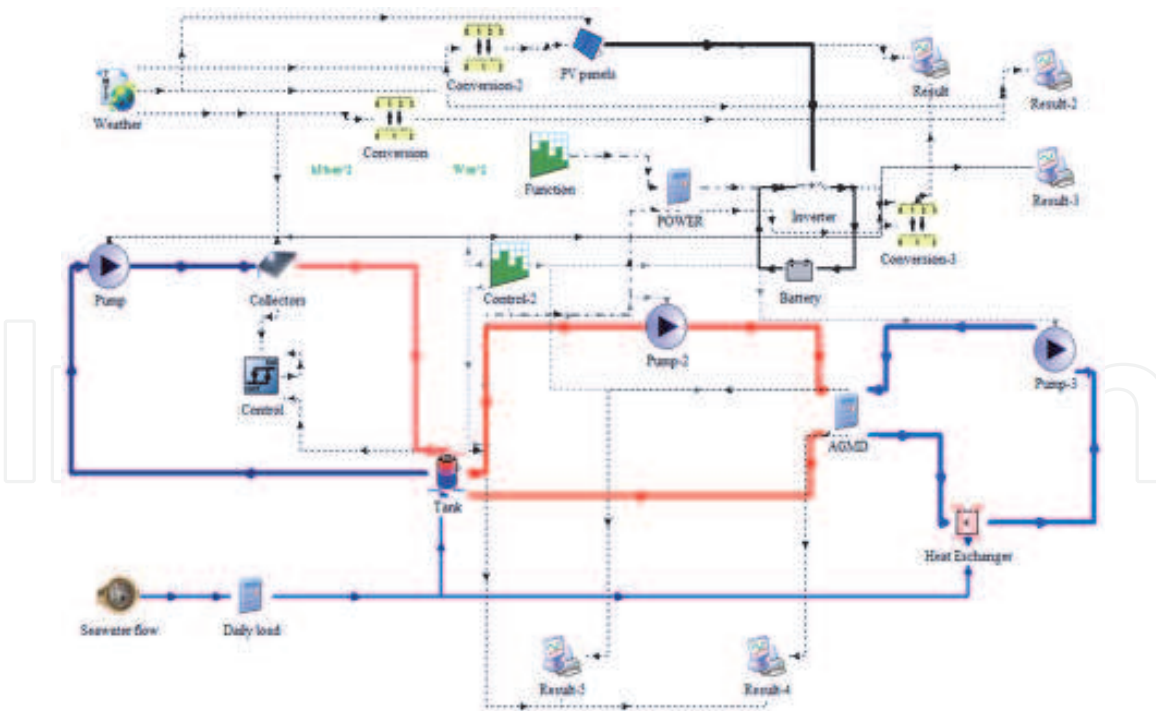
Figure 9.
Assembly diagram of the AGMD system in the TRNSYS simulation.

systems simulation program. A TRNSYS simulation project consists in choosing a set of mathematical models of physical components (by relying either on existing models in the TRNSYS model libraries or by creating them) and in describing the interactions between these models. TRNSYS contains a large number of standard models (utilities, thermal storage, equipment, loads and structures, heat exchangers, hydraulics, regulators, electrical/photovoltaic components, solar collectors).

The main component of the model is the AGMD unit, which is represented by a new equation in TRNSYS. As shown in **Figure 9**, additional components to the model include TYPE109-TM2 reading and processing of meteorological data, Type 91 heat exchanger, Type 60 storage tank, Type 1 flat plate collector, Type 2 differential temperature controller, Type 3 single speed pump, Type 6 auxiliary heaters, Type 94 photovoltaic panels, Type 47 storage battery, Type 48 inverter, Type 14 forcing functions, Type 57 unit conversion, and Type 65 online plotter. **Tables 1–3** show the values of parameters that are used in the TRNSYS model.

5. Results and discussion

5.1 Weather data

This model is installed in Ain-Temouchent weather (latitude 35° 3′0″N, longitude 1° 1′0″E in Algeria). **Figure 10** shows changing climate conditions throughout the year:

The weather of the state Ain-Temouchent is pleasant, warm, and moderate in general. At an average temperature of 25.7°C, August is the hottest month of the year. At 10.8°C on average, January is the coldest month of the year. Therefore, in this **Figure 10a**, we notice a change in temperature throughout the year, which reaches up to 40°C in the month of August, and we note that the wind is fairly moderate and does not exceed the speed of this one 15 m/s. For the irradiation, it

(a)

(b)
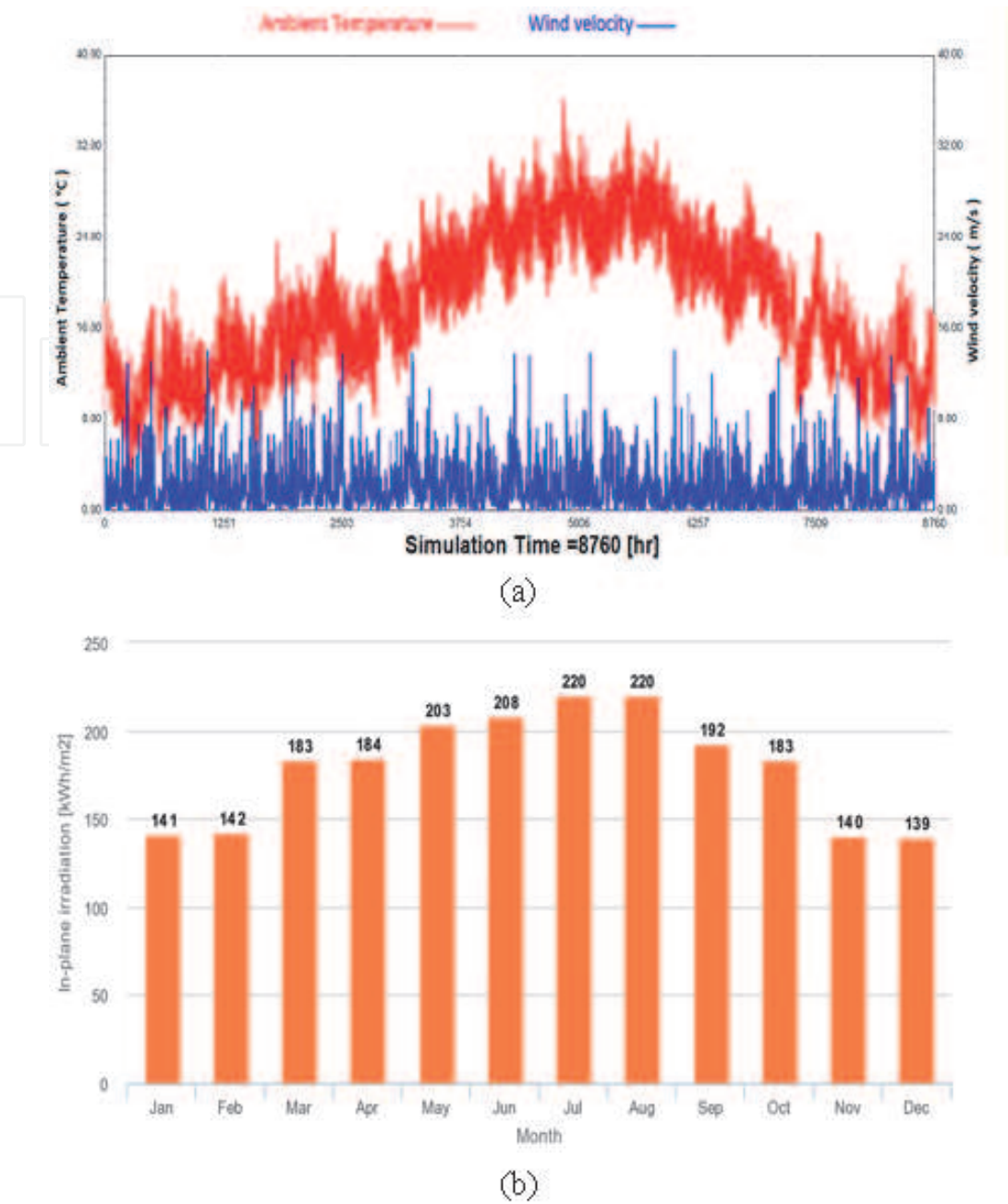
Figure 10.
(a) Ambient temperature, wind speed, and (b) irradiation in the Ain-Temouchent weather.

changes during the months of the year and reaches up to 220 kWh/m² in the month of August and July, as shown in **Figure 10b**, because the temperature is high in this period of the year.

5.2 The outlet temperatures and the useful thermal energy Qu for FPC system

The change of outlet temperatures of collectors and storage tank for the thermal system without using an auxiliary heater is illustrated in **Figure 11** on day 1st of January and August. The results show that the temperature decreases in January that reaches between 51 and 79°C (tank storage and collectors), but it increases in August when the temperature is high and reaches between 59 and 87°C, respectively. This change is due to the change in ambient temperature and radiation in the daytime and their difference from month to month as shown in **Figure 10**.
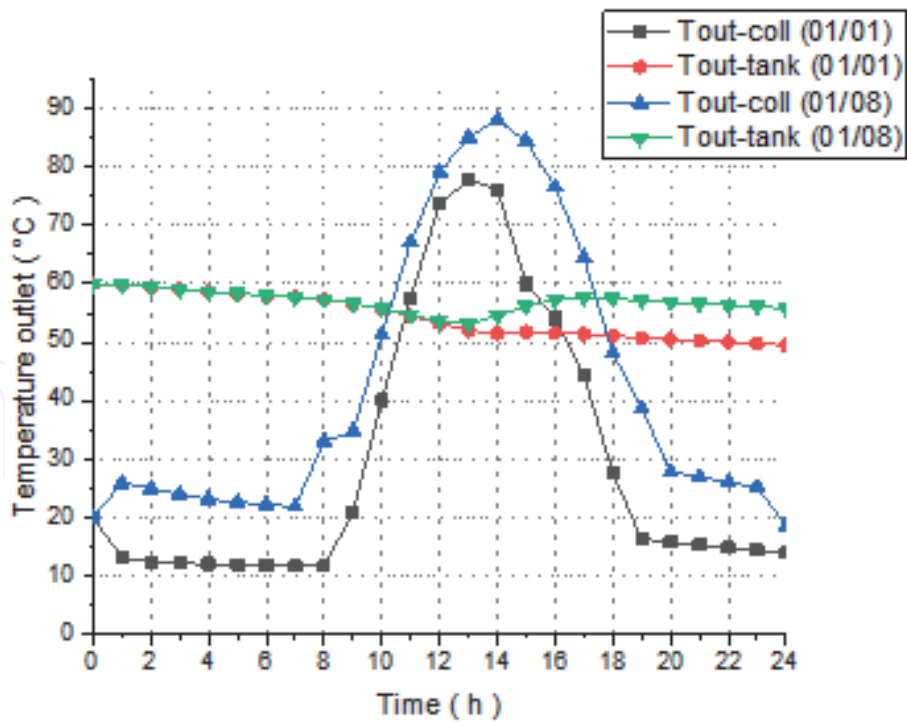
Figure 11.
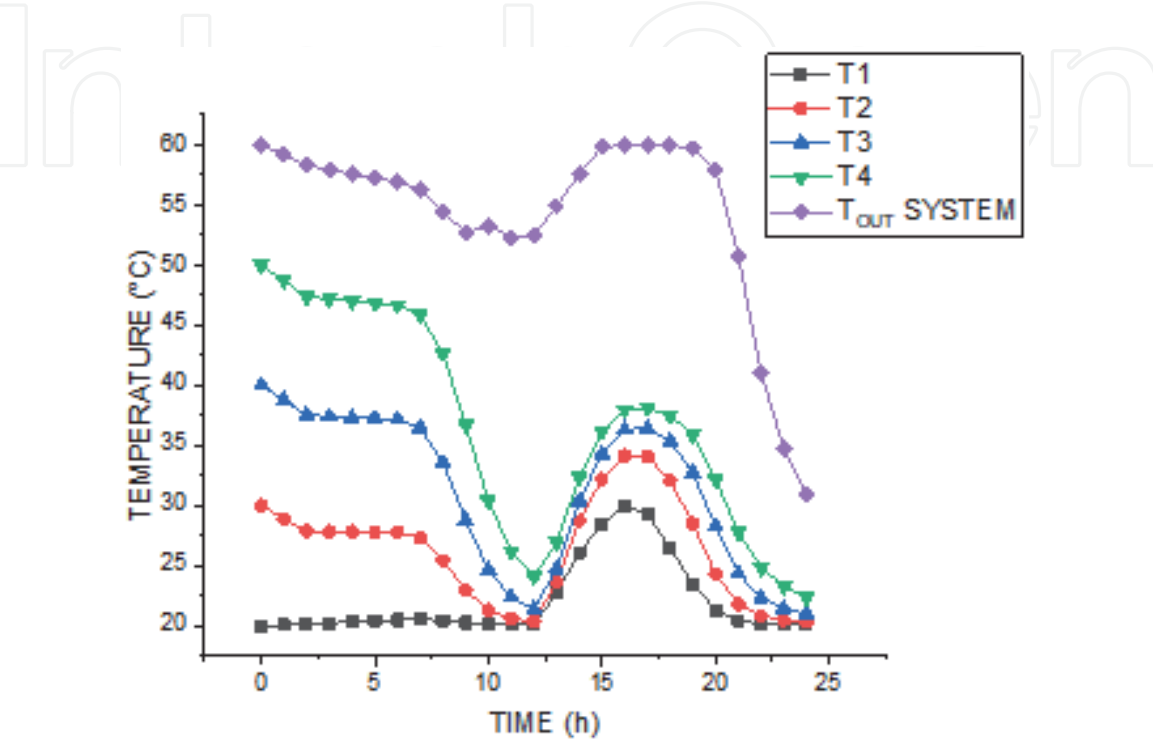*The outlet temperatures of the solar energy collector and hot water outlet tank.*

Figure 12 illustrates the amount of useful thermal energy obtained from collectors in different climatic conditions in January and August. We note that the productivity of the useful thermal energy is low in January and reaches 3250 kJ/hr. and increases in August, which reaches 3750 kJ/hr. Consequently, the changes in temperature and climatic conditions as clarified in **Figure 10** affect the useful thermal energy in different months selected. Therefore, when the temperature decreases, the useful thermal energy also decreases and vice versa.
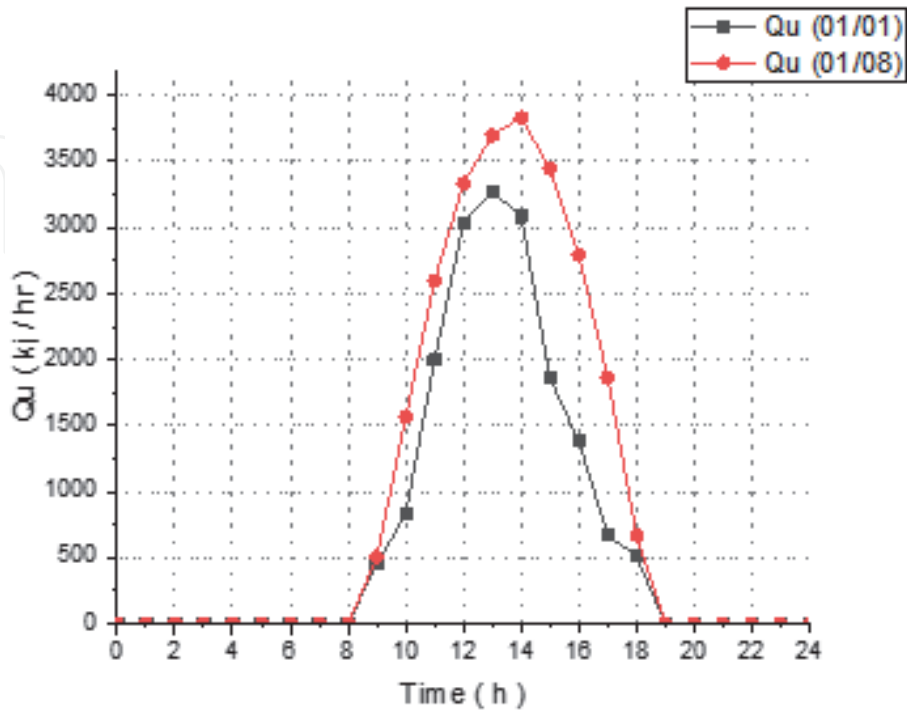
Figure 12.
The useful thermal energy Qu for FPC system.

5.3 The outlet temperatures in the storage tank

Figure 13 shows the temperature at the outlet of the storage tank at 60°C. In the storage tank, the initial temperature of the specified nodes into the tank's stratification (T1, T2, T3, T4, and T_{out} system) coming out from the heat exchanger in the tank has been calculated. They reach a maximum of 37°C on this first day of the cold month of January. For this reason, the auxiliary heater should be added to reach the temperature at 60°C when the weather temperature is low.

Figure 13.
The outlet temperatures in the storage tank for the FPC system.

5.4 Outlet cold and hot temperatures of the cooling system

Table 4 represents the changes of outlet cold and hot temperatures coming out of the heat exchanger (HX) at the heat transfer coefficient of the counter flow HX using the inlet temperatures between 20 and 50°C, respectively.

U A (kJ/hr. k) "Heat Exchanger"	Outlet hot temperature (°C)	Outlet cold temperature (°C)
100	28.87	41.16
150	26.56	43.47
200	25.20	44.82
250	24.31	45.72
300	23.68	46.35
350	23.21	46.82
400	22.85	47.18
500	22.32	47.70

U A, overall heat transfer coefficient of the counterflow heat exchanger.

Table 4.
Outlet cold and hot temperatures of the heat exchanger with (U A).

In order to improve the distillation membrane-cooling unit, the temperature changes and the overall heat transfer coefficient of the counter flow heat exchanger were calculated. We note that increasing the overall heat transfer coefficient increases the temperature on the cold side of the heat exchanger by 20 to 47.70°C. In addition, using the overall heat transfer coefficient (400–500 kJ/hr) is obtained the maximum production of distilled water in the membrane distillation process.

In **Figure 14**, the temperature coming from the distillation membrane is the same as the temperature entering the heat exchanger. This curve shows that the temperature of the distillation membrane reduces from 50 to 22.32°C in the hot side and increases from 20 to 47.7°C in the cold side. Therefore, the temperature of the hot side from the heat exchanger is reverse on the cold side.
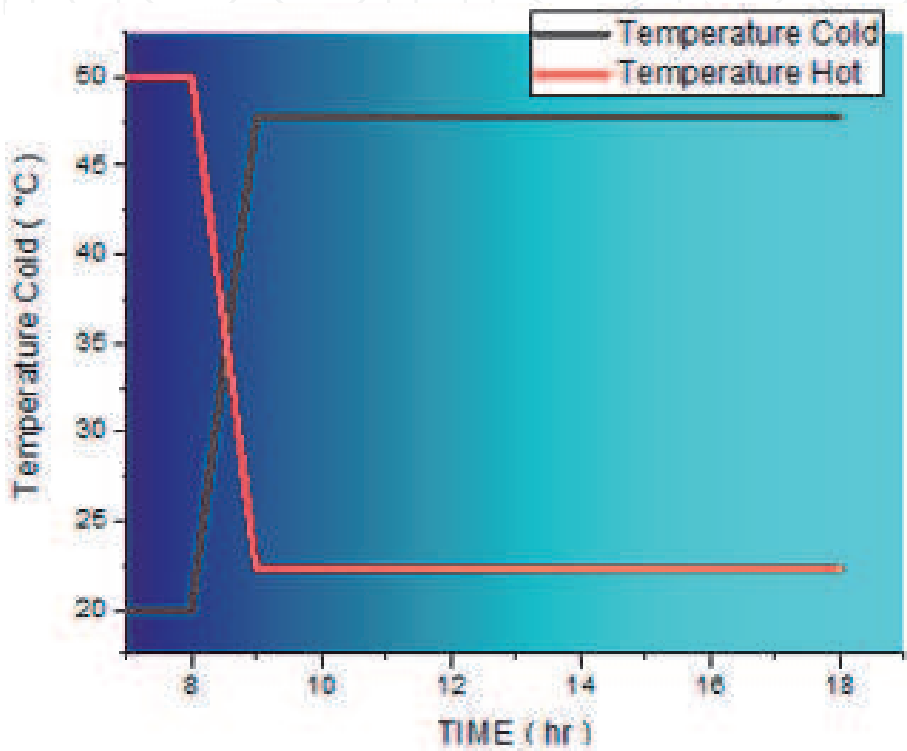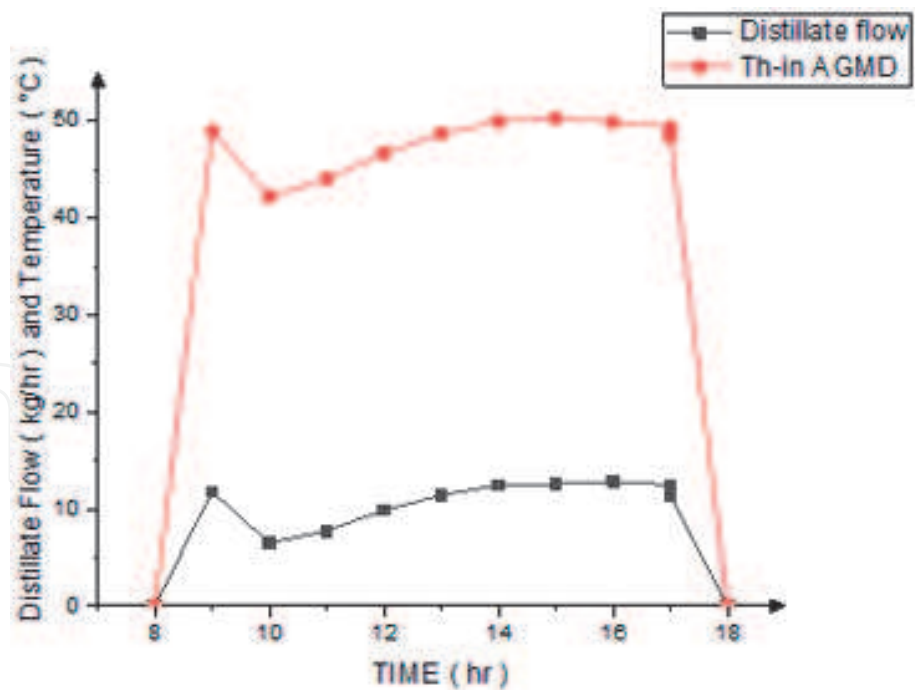

Figure 14.
Outlet cold and hot temperatures of the cooling system.

5.5 The inlet temperatures and distillate water flows of the AGMD module

Figure 15 presents the inlet temperatures and distillate water flows of the AGMD module on the day of 1st January. The MD solar systems are studied numerically using and including both flat plate collectors and photovoltaic panels. Therefore, the power load of solar AGMD systems is calculated and compared for the production of 100 L/day of distillate water. It was found that the developed system obtains an average distillate water flow that reaches 10 kg/hr. at the feed inlet temperature of AGMD module 52°C.

5.6 The daily power consumption and variations of energy of the PV panels

To save costs, a photovoltaic system is used based on renewable energy (solar energy). Therefore, the energy needed calculates for the pumps and replaces by four photovoltaic panels, each one has an area of 1.6 m^2 by using a TRNSYS help program.

Figure 15.
The inlet temperatures and distillate water flows of the AGMD module.

Estimated electricity requirements (kWh/day): The daily power consumption [or daily requirement in (kWh/day)] is given by the product of the nominal power of the load (kW) and the number of hours of daily use (hr/day). The daily power consumption is shown in **Table 5**.

Devices	Number	Unit power	Frequency or duration of daily use	Power	Energy
Pump of water	1	0.1 kW	10 h	0.1 kW	1 kWh
Pump of collectors	1	0.1 kW	10 h	0.1 kW	1 kWh
Pump of AGMD	1	0.1 kW	10 h	0.1 kW	1 kWh
Pump of cooling system	1	0.1 kW	10 h	0.1 kW	1 Kwh
Heat exchanger of cooling system	1	0.37 kW	10 h	0.37 kW	3.7 kWh
Total				0.77 kW	7.7 kWh

Table 5.
*The daily power consumption (water consumption profile 100 L/day).*

As shown in **Table 6**, increasing the daily power consumption increased the number of PV panels for AGMD process. Therefore, the various solar thermal systems of the MD process should be investigated to find the developed system that consumes less energy and with an average distillate water flow reaches 10 kg/hr. at the feed inlet temperature of AGMD module 52°C.

5.7 The various solar thermal systems of the MD process

Figure 16 presents a new approach for a numerical study to investigate the various solar thermal systems of the MD process: (1) tank storage with auxiliary heaters, (2) tank storage with two auxiliary heaters, (3) tank storage with a heat exchanger and without auxiliary heaters, and (4) tank storage with a heat exchanger and auxiliary

Total energy	PV panels
10.1 kWh	7 Panels
9.1 kWh	6 Panels
8.1 kWh	5 Panels
7.7 kWh	4 Panels

Table 6.
Variations of energy of the PV panels.
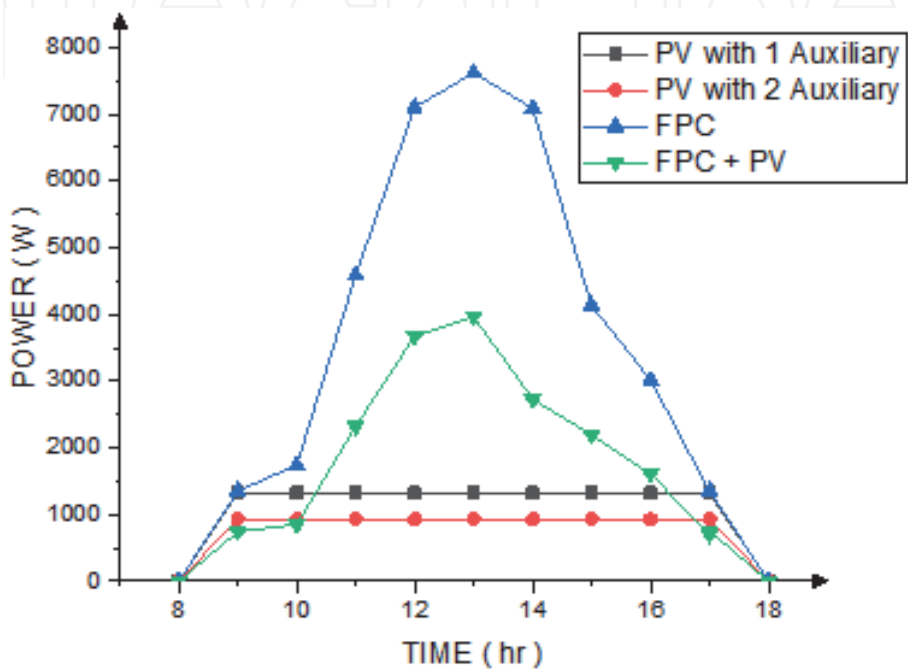
Figure 16.
Power to load of the auxiliary heaters of the thermal system for AGMD.

heaters. The various MD solar systems are studied numerically using and including both flat plate collectors and photovoltaic panels. Therefore, the power load of solar AGMD systems is calculated and compared for the production of 100 L/day of distillate water. It was found that the developed system in case (2) consumes less energy (1.2 kW) than other systems by percentage reaches 52.64% and with an average distillate water flow reaches 10 kg/hr. at the feed inlet temperature of AGMD module 52°C. Then, the developed system has been studied using TRNSYS and PVGIS programs on different days during the year in Ain Temouchent weather, Algeria.

6. Conclusion

A complete test rig to evaluate the performance of the membrane distillation module is driven by solar energy during the flat plate collectors heating process is simulated in Ain-Temouchent, Algeria.

The chapter presents a new approach for a numerical study to investigate the various solar thermal systems of the MD process: (1) tank storage with an auxiliary heater, (2) tank storage with two auxiliary heaters, (3) tank storage with a heat exchanger and without auxiliary heaters, and (4) tank storage with a heat exchanger and an auxiliary heater. The various MD solar systems are studied numerically using and including both flat plate collectors and photovoltaic panels.

Therefore, the power load of solar AGMD systems is calculated and compared for the production of 100 L/day of distillate water. It was found that the developed system in case (2) consumes less energy (1.2 kW) than other systems by percentage reach 52.64% and with an average distillate water flow reaches 10 kg/hr. at the feed inlet temperature of AGMD module 52°C. Then, the developed system has been studied using TRNSYS and PVGIS programs on different days during the year in Ain Temouchent weather, Algeria.

The simulation results show that a very simple AGMD system with a total collectors area of 4 m^2 for the production of 10 L/hr. of distilled water flow throughout the entire year. To save costs, a photovoltaic system is used depending on renewable energy (solar energy). Therefore, the energy needed is calculated for the pumps and is replaced by 4 photovoltaic panels, and each one has an area of 1.6 m^2 using an energy storage battery (12 V, 200 Ah) via TRNSYS and PVGIS to help programs. Accordingly, the purpose of this study is the use of solar panels in the photovoltaic system to produce the necessary electrical energy. The AGMD system using solar energy for seawater desalination will be useful for further simulations or applications of the technology. Finally, these systems of projects that integrate renewable energy technologies with additional services are in principle attractive in terms of the associated socioeconomic benefits.

Acknowledgements

Author details

Abdelfatah Marni Sandid[1]*, Taieb Nehari[1], Driss Nehari[2] and Yasser Elhenawy[3]

1 Smart Structures Laboratory (SSL), University Ain Temouchent Belhadj Bouchaib, Ain-Temouchent, Algeria

2 Department of Mechanical Engineering, University Ain Temouchent Belhadj Bouchaib, Ain-Temouchent, Algeria

3 Department of Mechanical Power Engineering, Port Said University, Port Said, Egypt

*Address all correspondence to: abdelfatahsandid@hotmail.com

IntechOpen

References

[1] Alkhudhiri A, Darwish N, Hilal N. Membrane distillation: A comprehensive review. Desalination. 2012;**287**:2-18. DOI: 10.1016/j. desal.2011.08.027

[2] Koschikowski J, Wieghaus M, Rommel M, Ortin S, Suarez P, Betancort-Rodríguez J. Experimental investigations on solar driven stand-alone membrane distillation systems for remote areas. Desalination. 2009;**248**: 125-131. DOI: 10.1016/j. desal.2008.05.047

[3] Zhani K, Zarzouma K, Ben-Bachaa H, Koschikowskic J, Pfeifle D. Autonomous solar powered membrane distillation systems: State of the art. Desalination and Water Treatment. 2016;**57**: 23038-23051. DOI: 10.1080/ 19443994.2015.1117821

[4] Chen YH, Li YW, Chang H. Optimal design and control of solar driven air gap membrane distillation desalination systems. Applied Energy. 2012;**100**: 193-204. DOI: 10.1016/j. apenergy.2012.03.003

[5] Marni-Sandid A, Bassyouni M, Nehari D, Elhenawy Y. Experimental and simulation study of multichannel air gap membrane distillation process with two types of solar collectors. Energy Conversion and Management. 2021;**243**: 1-14. DOI: 10.1016/j. enconman.2021.114431

[6] Marni-Sandid A, Nehari T, Nehari D. Simulation study of an air-gap membrane distillation system for seawater desalination using solar energy. Desalination and Water Treatment. 2021;**229**:40-51. DOI: 10.5004/dwt.2021.27394

[7] Marni-Sandid A, Nehari D, Elmeriah A, Remlaoui A. Dynamic simulation of an air-gap membrane distillation (AGMD) process using photovoltaic panels system and flat plate collectors. Journal of Thermal Engineering. 2021;**7**:117-133. DOI: 10.18186/thermal.870383

[8] Khayet M, Matsuura T. Introduction to Membrane Distillation. Book of Membrane Distillation; 2011. 1–16 p. DOI:10.1016/b978-0-444-53126- 1.10001-6

[9] Ruh U, Majeda K, Richard J, James T, McLeskey J, Mohammad A, et al. Energy efficiency of direct contact membrane distillation. Desalination. 2018;**433**:56-67. DOI: 10.1016/j. desal.2018.01.025

[10] Qtaishata M, Matsuura T, Kruczek B, Khayet M. Heat and mass transfer analysis in direct contact membrane distillation. Desalination. 2008;219:272-292. DIO:10.1016/j. desal.2007.05.019

[11] Hassler GL. U.S. patent US3129146A [14 April 1964]

[12] Weyl PK. U.S. patent US3340186A [5 September 1967]

[13] Jonsson S, Wimmerstedt R, Harrysson C. Membrane distillation: A theoretical study of evaporation through microporous membranes. Desalination. 1985;**56**:237. DOI: 10.1016/0011-9164 (85)85028-1

[14] Gostoli C, Sarti GC, Matulli S. Low temperature distillation through hydrophobic membranes. Journal of Separation and Purification Technology. 1987;**22**:855. DOI: 10.1080/ 01496398708068986

[15] Banat FA, Al-Rub FA, Jumah R, Shannag M. Theoretical investigation of membrane distillation role in breaking the formic acid-water azeotropic point: Comparison between Fickian and Stefan-Maxwell-based models.

International Communications in Heat and Mass Transfer. 1999;**26**(6):879-888. DOI: 10.1016/s0735-1933(99)00076-7

[16] Hanemaaijer JH, van Medevoort J, Jansen AE, Dotremont C, Van-Sonsbeek E, Yuan T, et al. Memstill membrane distillation – A future desalination technology. Desalination. 2006;**199**: 175-176. DOI: 10.1016/j. desal.2006.03.163

[17] Vandita T, Shahu B, Thombre S. Air gap membrane distillation: A review. Journal of Renewable and Sustainable Energy. 2019;**11**:45901. DOI: 10.1063/ 1.5063766

[18] Duong HC, Cooper P, Nelemans B, Cath TY, Nghiem LD. Evaluating energy consumption of air gap membrane distillation for seawater desalination at pilot scale level. Journal of Separation and Purification Technology. 2016;**166**: 55. DOI: 10.1016/j.seppur.2016.04.014

[19] Minier-Matar J, Hussain A, Janson A, Benyahia F, Adham S. Field evaluation of membrane distillation technologies for desalination of highly saline brines. Desalination. 2014;**351**: 101-108. DOI: 10.1016/j. desal.2014.07.027

[20] Swaminathana J, Chunga HW, Warsingera DM, AlMarzooqib FA, Arafatb HA. Energy efficiency of permeate gap and novel conductive gap membrane distillation. Journal of Membrane Science. 2016;**502**:171-178. DOI: 10.1016/j.memsci.2015.12.017

[21] Alklaibi AM, Lior N. Membrane-distillation desalination: Status and potential. Desalination. 2005;**171**(2): 111-131. DOI: 10.1016/j. desal.2004.03.024

[22] Camacho L, Dumée L, Zhang J, Li J, Duke M, Gomez J, et al. Advances in membrane distillation for water desalination and purification

applications. Water. 2013;**5**(1):94-196. DOI: 10.3390/w5010094

[23] Chafidz A, Esa DK, Irfan W, Yasir K, Abdelhamid A, Saeed A. Design and fabrication of a portable and hybrid solar-powered membrane distillation system. Journal of Cleaner Production. 2016;**133**:631-647. DOI: 10.1016/j. jclepro.2016.05.127

[24] Uday KN, Martin A. Experimental modeling of an air-gap membrane distillation module and simulation of a solar thermal integrated system for water purification. Desalination and Water Treatment. 2017;**84**:123-134. DOI: 10.5004/dwt.2017.21201